Pergamon

Available online at www.sciencedirect.com
SCIENCE DIRECT®

Cement and Concrete Research 33 (2003) 1189–1202

CEMENT AND CONCRETE RESEARCH

Compressive strength and hydration of wastepaper sludge ash–ground granulated blastfurnace slag blended pastes

J. Bai[a], A. Chaipanich[a], J.M. Kinuthia[a], M. O'Farrell[a], B.B. Sabir[a], S. Wild[a,*], M.H. Lewis[b]

[a]*School of Technology, University of Glamorgan, Pontypridd CF37 1DL, UK*
[b]*Department of Physics, University of Warwick, Coventry CV4 7AL, UK*

Received 20 October 2001; accepted 21 January 2003

Abstract

Compressive strength and hydration characteristics of wastepaper sludge ash–ground granulated blastfurnace slag (WSA–GGBS) blended pastes were investigated at a water to binder (w/b) ratio of 0.5. The strength results are compared to those of normal Portland cement (PC) paste and relative strengths are reported. Early relative strengths (1 day) of WSA–GGBS pastes were very low but a marked gain in relative strength occurred between 1 and 7 days and this increased further after 28 and 90 days. For the 50% WSA–50% GGBS blended paste, the strength achieved at 90 days was nearly 50% of that of the PC control paste. Transmission electron microscopy (TEM), X-ray diffraction (XRD) and thermogravimetric (TG) analysis were carried out to identify the mineral components in the WSA and the hydration products of WSA and WSA–GGBS pastes. The principal crystalline components in the WSA are gehlenite, calcium oxide, bredigite and α'-C_2S (stabilised with Al and Mg) together with small amounts of anorthite and calcium carbonate and traces of calcium hydroxide and quartz. The α'-C_2S and bredigite, which phase separate from liquid phase that forms a glass on cooling, are difficult to distinguish by XRD. The hydration products identified in WSA paste are CH, C_4AH_{13}, $C_3A.0.5C\bar{C}.0.5CH.H_{11.5}$ and C-S-H gel plus possible evidence of small amounts of C_2ASH_8 and $C_3A.3C\underline{S}.H_{32}$. Based upon the findings, a hydration mechanism is presented, and a model is proposed to explain the observed strength development.

Keywords: Amorphous material; Hydration products; Compressive strength; Physical properties; Blended cement

1. Introduction

Annual paper consumption in the UK (some of which is imported) is around 13 million tonnes and the source of much of this is from recovered paper [1]. Over the past two decades, the use of recovered paper by the UK paper industry has gradually increased to an annual amount (1999) of about 5 million tonnes. The amount of recovered paper used as a proportion of the total output from paper mills (the utilisation rate) for the UK is 72%, which is one of the highest in the world. The figure varies substantially depending on the paper sector. For newsprint, it is around 100%. When paper is recycled, the part of the paper that is not recovered includes the inorganic coatings and fillers (calcite and kaolin) plus residual cellulose fibres [1–6]. It comprises a sludge that in some cases is incinerated and is normally dumped to landfill or disposed of by land spread [2,3]. These methods of disposal are expensive and cause concern by their impact on the environment. According to Frederick et al. [4], an economical alternative to landfill disposal is either recovery of energy from the sludge, reuse of materials from the sludge or both. For example, Pera and Amrouz [2] have shown that highly reactive metakaolin, which is a high-added-value product, can be produced from paper sludge by calcining at 700 °C to 750 °C for 2 to 5 h. Under these conditions, the organics in the sludge are destroyed, but decarbonation of the calcite is prevented. Thus, when combined with Portland cement (PC) and water, the calcite reacts with the lime and metakaolin to produce monocarboaluminate and C-S-H gel.

Aylesford Newsprint, which is the UK's principal wastepaper recycling company for the production of newsprint, combusts wastepaper sludge in a fluidised bed and generates steam for use in the plant. The ash resulting from combustion of the sludge (about 700 tonnes/week) is then dumped

* Corresponding author. Tel.: +44-1443-482142; fax: +44-1443-482169.
E-mail address: swild@glam.ac.uk (S. Wild).

0008-8846/03/$ – see front matter © 2003 Elsevier Science Ltd. All rights reserved.
doi:10.1016/S0008-8846(03)00042-5

Table 1
Oxide composition of the WSA

Oxide	%
SiO_2	25.70
Al_2O_3	18.86
Fe_2O_3	0.87
CaO	43.51
MgO	5.15
Na_2O	1.56
K_2O	1.31
Li_2O	0.01
P_2O_5	0.52
TiO_2	0.68
MnO	0.04
BaO	0.04
SrO	0.09
SO_3	1.05
LOI	1.2
Total	100.59

Analytical data supplied by Southern Water for Aylesford Newsprint, 11 July 2000.

to landfill [6]. The sludge remains in the combustion zone for 3–5 s at temperatures between 850 and 1200 °C and is then cooled rapidly (in about 3–5 s) to 200 °C to prevent the formation of dioxins. The process, which is very different from that described above [2], is similar to the flash calcining of kaolinite [7]. In a preliminary study, Kinuthia et al. [6] analysed wastepaper sludge ash (WSA) produced by Aylesford Newsprint. They used chemical analysis to determine principal oxides, X-ray diffraction (XRD) analysis to identify crystalline phases and thermogravimetric (TG) analysis to follow the hydration for WSA–ground granulated blastfurnace slag (GGBS) blends. The crystalline phases identified in the WSA were quartz, gehlenite, anorthite, calcite and quicklime, the quartz being mainly derived from the fluidised bed material. The authors also suggested, from the results of chemical analysis, that the WSA may have quite a high amorphous silica and alumina content. The TG analysis of the hydration products from WSA–GGBS blends was inconclusive, identifying C-S-H gel and ettringite and possible formation of carboaluminate phases, gehlenite hydrate and hydrogarnet. The authors [6] concluded that hydration of WSA does take place, but the hydration mechanism and the degree to which hydration products are derived from pozzolanic reactions or from direct hydration of components in the WSA was not established. The current study investigates the use of WSA, resulting from the combustion of the sludge, as a cementitious material and attempts to answer some of these questions.

Table 2
Principal oxides released from WSA and insoluble residue (test complying with BS 1881 Part 124)

Component	%
Insoluble residue	14.80
Soluble silica	22.55
Soluble calcium oxide	40.90
Soluble sulphate as SO_3	0.83
CO_2	2.32
Soluble Al_2O_3	15.60
Soluble MgO	2.30
Soluble Fe_2O_3	0.66
Total	99.96

Table 3
Major oxide components and physical properties of PC and GGBS

	PC	GGBS
Oxide composition (%)		
SiO_2	21.00	35.50
Al_2O_3	4.63	12.00
Fe_2O_3	2.26	0.40
CaO	65.60	42.0
MgO	1.18	8.00
SO_3	2.69	0.20
Na_2O	0.16	–
K_2O	0.78	–
Physical properties		
Density (kg/m^3)	3150	2800
Blaine specific surface (m^2/kg)	380	510

2. Materials

The WSA was supplied by Aylesford Newsprint as a 550-kg batch collected from the flue gases of the wastepaper sludge combustor. The original sludge comprised about one-third kaolinite, one-third calcium carbonate and one-third cellulose fibre. Duplicate samples were taken from the batch for analysis. It should be noted that the WSA in this work, although from the same source as that reported in Ref. [6], did not contain the coarser bottom ash, which is contaminated with quartz from the fluidised bed. Table 1 gives the oxide composition of the ash. Each value is the average of the duplicate determinations. In order to assess the reactivity of the WSA, the samples were also tested in compliance with BS 1881 Part 124, which is the test for determining the cement content in concrete. The results (see Table 2) also include determination of the amount of CO_2 as carbonate. Assuming that the CO_2 is bound as $CaCO_3$ in the WSA, then the calcium carbonate content of the WSA is approximately 5 wt.%. In addition, the free lime (CaO) content, which was determined in accordance with BS EN 196-2 [8], is also about 5 wt.%. The specific surface of the WSA, determined using a Mastersizer 2000 unit, is 410 m^2/kg (average value from 51 samples) and the material density,

Table 4
Soundness test results

Mix code	Soundness (expansion; mm)
PC	0.5
WSA	6
W40G60	1.2
W50G50	1.2
W60G40	1.4

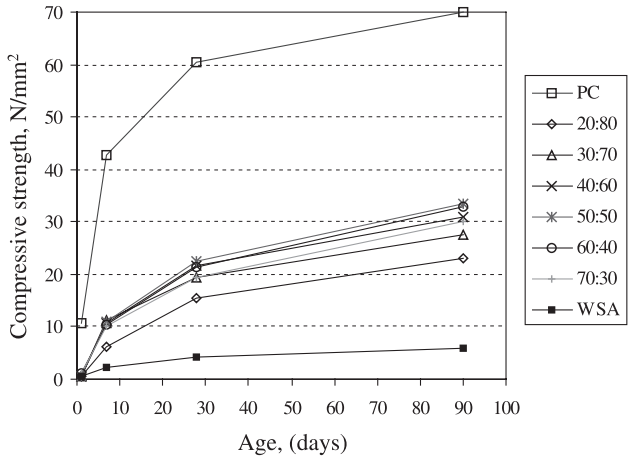

Fig. 1. Strength development of PC, WSA–GGBS and WSA pastes (w/b = 0.5).

determined using a displacement method with paraffin, is 2520 kg/m^3. The GGBS used in this investigation was supplied by Civil and Marine Slag Cement. A normal 42.5 N PC, complying with BS 12 [9] supplied by Rugby Group, was used for the control mixes. The physical and chemical characteristics of the PC and GGBS are given in Table 3. In addition, gypsum was used as direct weight replacement of the total WSA content at 5% and 10% in order to characterise ettringite phase development from DTG and XRD of WSA pastes.

3. Experimental details

3.1. Specimen preparation

3.1.1. Soundness

The presence of free lime (CaO) in the WSA is likely to produce unsoundness, in that 'slaked' lime occupies a larger volume than quicklime, promoting expansion which, if occurring after setting, results in unsoundness. Thus, the Le Chatelier test prescribed by EN 196-3 [10] was conducted on the control PC paste, on the WSA paste and on some of the WSA–GGBS blended pastes at standard consistence. Unsoundness is indicated if expansion of the paste, under the test procedures specified, exceeds 10 mm.

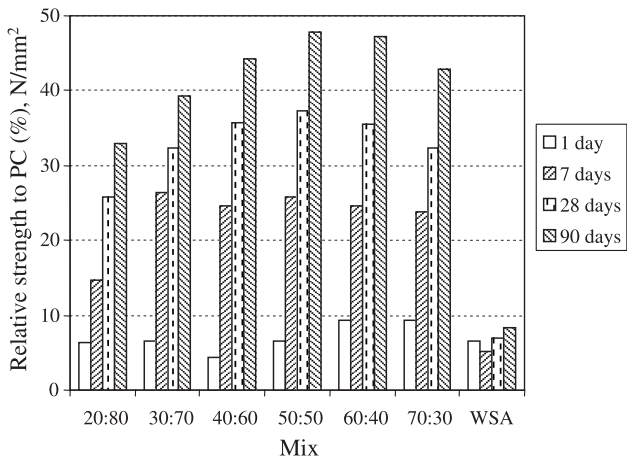

Fig. 2. Compressive strength of WSA–GGBS and WSA pastes relative to PC strength (w/b = 0.5).

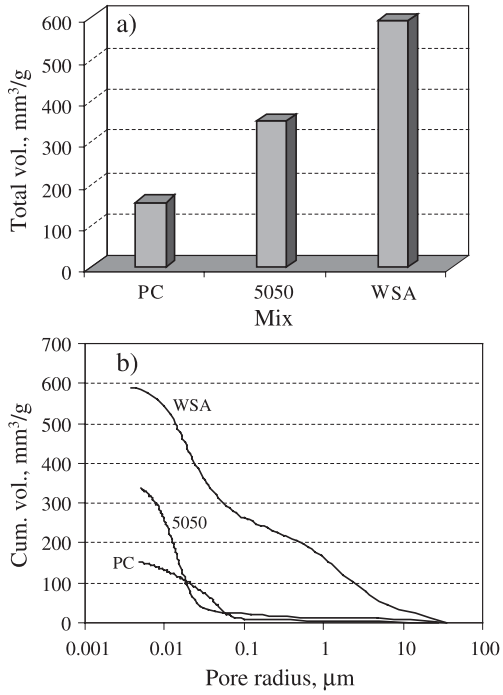

Fig. 3. Pore structure of PC, WSA and 50% WSA–50% GGBS pastes cured for 28 days.

3.1.2. Strength testing

A number of WSA–GGBS blends were prepared with WSA to GGBS ratios of 20:80, 30:70, 40:60, 50:50, 60:40 and 70:30. In addition, 100% WSA and 100% PC were used as controls. For the blends, batches of 1 kg were prepared by intergrinding the appropriate quantities of WSA and GGBS together for 1 min in a Mixermill 2000 unit to ensure homogeneity. The pastes were mixed using a mixer similar to that specified by BS EN 196-1 [11] but of a larger size, and the mixing procedure was carried out in accordance with BS EN 196-3 [10]. A water to binder (w/b) ratio of 0.5 was used for all mixes. This was chosen as an optimum value, in that below this, pastes with high WSA content were completely unworkable, and above this, pastes with

Table 5
Threshold radii and pore fineness for PC, 50% WSA–50% GGBS and WSA pastes

Parameter	PC	50% WSA–50% GGBS	WSA
Threshold radius (μm)	0.07	0.02	6
% of pore space occupied by pores of radius < 0.05 μm	75	93	48

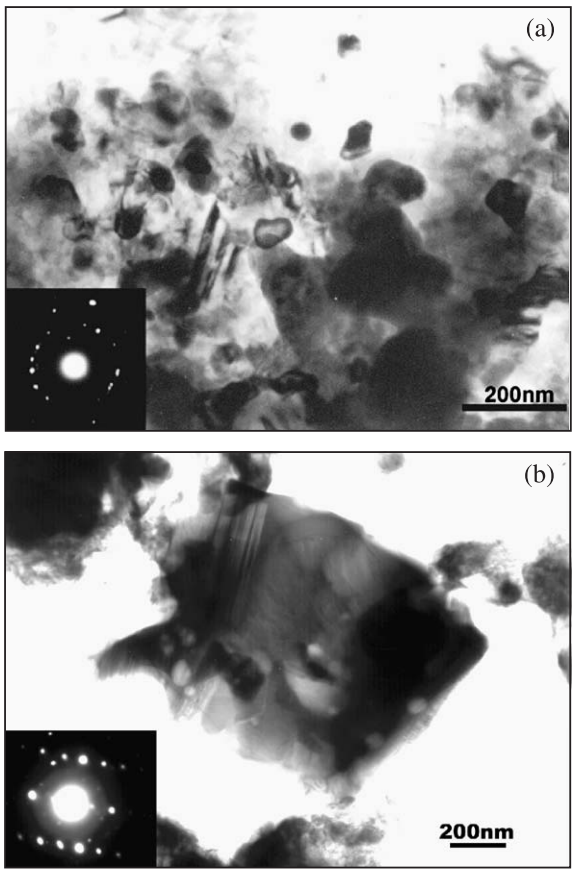

Fig. 4. TEM micrograph of (a) small and (b) large crystals in WSA.

high GGBS contents were very fluid. Paste specimens were cast in 50-mm standard cube moulds, vibrated to ensure good compaction and demoulded after 24 h. Because of the very low workability of high-WSA mixtures (see Ref. [6]), manual compaction combined with vibration was required to fully compact the mixtures. The specimens were then cured in water at 20 °C and were tested in compression at 1, 7, 28 and 90 days. For each curing period, three specimens were tested at a loading rate of 0.3 $N/mm^2/s$.

3.1.3. Porosity and pore size distribution

Small samples ($\sim$10 g) were taken from the centres of the fractured cubes and dried to constant weight in a desiccator (over carbosorb to prevent carbonation and silica gel to reduce relative humidity) at 45 °C. When dried, the pore structures of pieces from selected pastes (WSA, 50% WSA–50% GGBS and PC) were investigated by mercury porosimetry using a Fisons Instruments Macropore Unit 120 and Porosimeter 2000WS.

3.2. Analysis

3.2.1. Analysis of WSA

In order to identify and characterise crystalline phases in the WSA, the dry powder samples were subjected to XRD analysis using a Phillips diffractometer PW1965 and a generator PW1730 with a graphite monochromator and Cu Kα radiation. To characterise any amorphous phases and to complement the XRD analysis of crystalline phases, the WSA powder was examined by transmission electron microscopy (TEM) in a JEOL 2000FX microscope linked to an Oxford eXL EDAX system. TEM samples were prepared by suspending the WSA powder in a methyl acetate colloidon solution. A drop of the solution was then placed on a carbon-coated copper grid and evaporated, leaving particles trapped on the grid. Some of the particles were sufficiently thin to be transparent to the electron beam and could therefore be imaged and analysed by TEM. Particles were analysed using the EDAX system. It is appreciated that in using this method of sample preparation, samples may not be truly representative of the whole powder, therefore several grids were made up from samples taken from different parts of the WSA powder sample. Samples were also examined and analysed by SEM (JEOL 6100) to improve the sampling statistics.

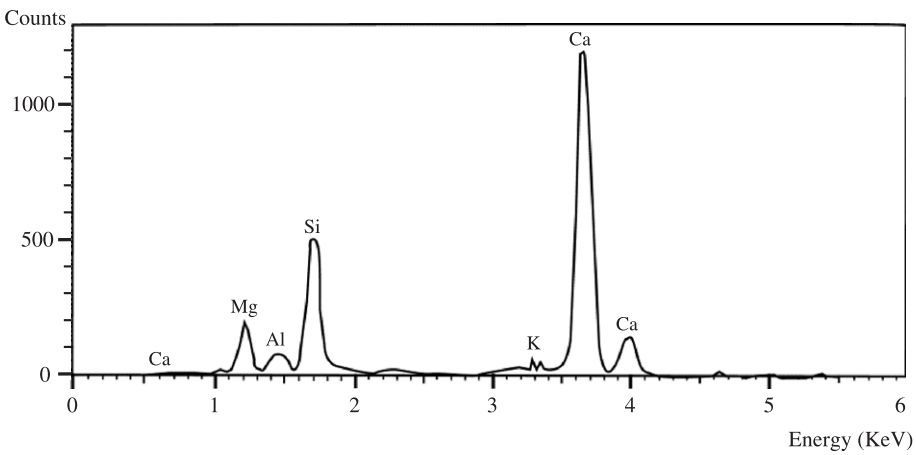

Fig. 5. Typical EDAX analysis of small crystals.

Table 6
EDAX analyses of small crystals (atomic percent)

Crystal no.	Ca	Si	Al	Mg	Fe	S
1	54.11	24.05	2.56	17.29	0.67	0.89
2	60.73	21.89	2.82	12.22	1.39	0.9
3	57.66	21.19	2.32	15.05	0.42	3.38
4	52.95	25.46	3.71	15.87	1.05	0.98
5	52.91	26.08	3.15	15.81	0.92	0.75
6	56.08	24.07	2.28	17.06	0.34	0.34
Mean	55.74	23.79	2.81	15.55	0.80	1.21
7	61.57	19.69	17.87	0.48	0.26	0.40
8	51.95	22.63	22.83	1.17	1.13	0.25
9	62.26	17.74	14.07	2.25	0.38	3.31
Mean	58.6	20.02	18.26	1.30	0.59	1.32

Table 7
EDAX analyses of large crystals (atomic percent)

Crystal no.	Ca	Si	Al	Mg	Fe	S
1	43.02	27.31	25.16	3.13	0.94	0.11
2	39.01	30.51	26.12	2.06	0.47	0.01
3	39.11	30.52	26.14	2.03	0.40	0.01
4	41.29	28.32	24.64	4.12	1.06	0.25
5	43.43	32.54	21.76	0.84	0.52	0.12
6	37.03	30.43	28.14	2.41	0.42	0.12
7	30.00	28.26	23.50	3.21	2.27	1.43
8	33.34	33.21	25.32	6.15	0.73	0.57
9	33.56	34.24	24.39	5.43	0.66	0.59
Mean	38.75	30.59	25.02	3.26	0.83	0.36

3.2.2. Analysis of hydration products

Dried pieces from the fractured cubes were ground to a fine powder and samples of about 5 mg were then subjected to temperatures of up to 1000 °C in a TA Instruments TGA 2950 thermogravimetric analyser, and the weight loss–temperature (TG) and derivative weight loss–temperature (DTG) profiles recorded. In addition, XRD analysis was carried out on the hydrated material to characterise the crystalline phases.

4. Results and discussion

4.1. Physical properties

4.1.1. Soundness

The expansions of the different pastes are shown in Table 4. Clearly, although the WSA paste expansion does not exceed the specified 10-mm limit, the paste is much less sound than the other pastes. In particular, combining WSA with GGBS substantially improves soundness and gives expansion values tending towards that of PC.

4.1.2. Compressive strength

Compressive strength results of PC, WSA–GGBS and WSA pastes, cured for up to 90 days, are given in Fig. 1. The compressive strengths of WSA–GGBS and WSA pastes are lower than that of the PC paste at all ages, and WSA paste shows particularly low strength development up to 28 days (4 MPa compared to 61 MPa for PC paste). The relative strengths (strength of paste ÷ strength of PC paste at same age) are given in Fig. 2. It is clear that blending WSA with GGBS results in enhanced strengths at all curing ages and the optimum composition to give maximum strength occurs at around 50% WSA–50% GGBS, for which the 90-day strength is nearly 50% of the PC control strength.

4.1.3. Porosity and pore size distribution

Fig. 3 shows the total pore volume and the cumulative pore volume versus pore radius for 28-day cured PC, WSA and 50% WSA–50% GGBS pastes. Blending the WSA with GGBS substantially reduces pore volume (Fig. 3a), although not to the level exhibited by the PC paste. However, more significantly, blending WSA with GGBS produces very substantial pore refinement (Fig. 3b) and produces a pore structure finer than that of the PC paste. This is confirmed by the data presented in Table 5, which gives values of

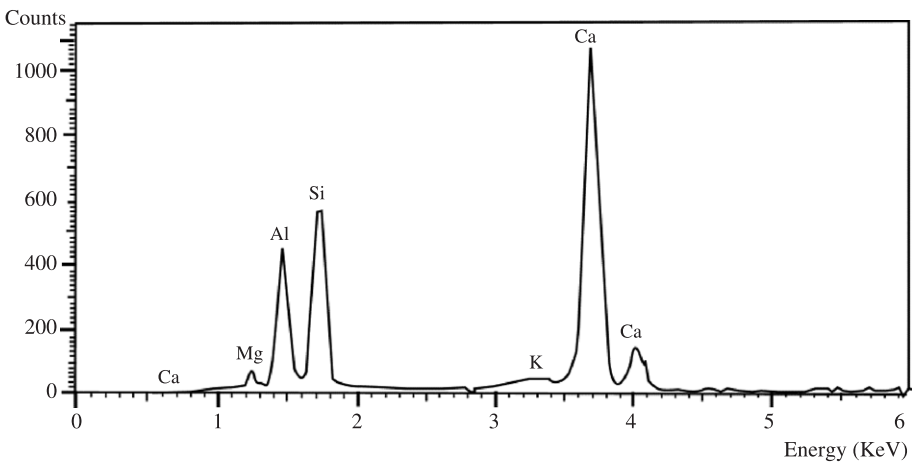

Fig. 6. Typical EDAX analysis of large crystals.

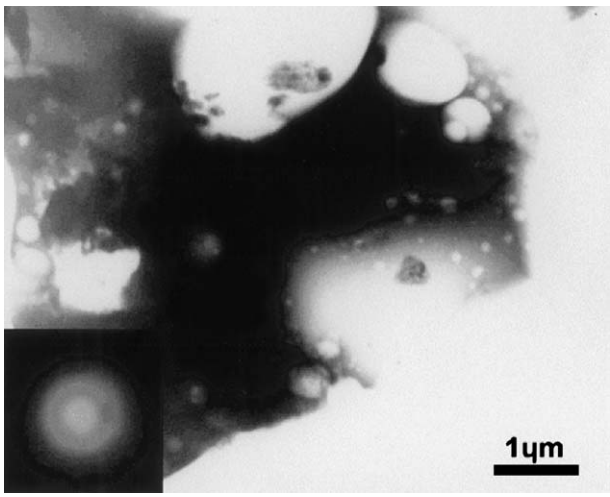

Fig. 7. TEM micrograph of amorphous glassy particles.

threshold radii and also the percentage of fine pores (radii <0.05 μm) for the three pastes.

4.2. Analytical results

4.2.1. Characterisation of WSA using TEM and XRD

TEM studies of the different types of particles comprising the WSA show that the ash is very finely crystalline with some small 'glassy' regions made up of phase separated spherical glass particles. The overall particle morphology suggests the presence of two crystalline phases, and these are loosely classified as 'small' crystals (mean Feret diameter 71 nm [S.D. ± 14 nm]) and 'large' crystals. Fig. 4a shows a TEM micrograph of the small crystals and Fig. 5 shows a typical EDAX analysis. The small crystals (Table 6) in fact appear to consist of two separate phases. One phase contains a significant amount of magnesium but very little aluminium and has a cation composition ($Ca_7Mg_2Si_3$) similar to that reported by Taylor [13] for bredigite (Ca_7MgSi_4), but with increased Mg and reduced Si. The other phase approximates to an Al-substituted dicalcium silicate phase. Presumably the two intimately associated phases arise as a result of phase separation from the liquid, with the Mg principally going into the bredigite-type phase and the Al going into the dicalcium-silicate-type phase.

Fig. 4b shows a TEM micrograph of fragments of a large crystal and Fig. 6 shows a typical EDAX analysis. The large crystals are essentially calcium aluminosilicate crystals containing small amounts of Mg and minor amounts of S, Fe and K. There is a much smaller degree of variability in the cation compositions of these crystals and (neglecting the minor elements) an average of nine analyses gives (see Table 7) a cation composition of $Ca_2Al_{1.29}Si_{1.58}Mg_{0.16}$. This cation composition is similar to that of gehlenite Ca_2Al_2Si but is silicon rich, aluminium deficient, and may be rewritten as $Ca_2(Al_{1.29}Si_{0.58}Mg_{0.16})Si$.

Fig. 7 shows a TEM micrograph of the amorphous glassy particles, which range in size from 5 to 10 μm in diameter, and Fig. 8 shows an example of an EDAX analysis of one of the particles. Their composition (Table 8) shows quite a wide variation in Ca level although the Si/Al ratios fall within a relatively narrow range. Table 8 shows the mean oxide composition of the glassy phase, which has a silica/alumina ratio of 1.46. This is close to that of 1.36 for the WSA (Table 1) and reflects the SiO_2/Al_2O_3 ratio of the original kaolinite in the paper sludge. The glassy phase has a mean composition that falls within the typical slag composition range (Table 9) but at the low-calcia, high-alumina end of the range, suggesting that it will be of relatively low hydraulicity. The approximate proportion of glassy material, judged from SEM images of WSA powder, is less than 20%. No evidence of any particles of metakaolin was observed in the TEM study.

XRD analysis (Fig. 9) shows that the crystalline phases making up the WSA are gehlenite, which gives the strongest diffraction pattern (peaks G), together with calcium oxide or quicklime (characterised by peaks Q at 2.76, 2.40 and 1.70 Å), a small amount of which has hydrated to give $Ca(OH)_2$

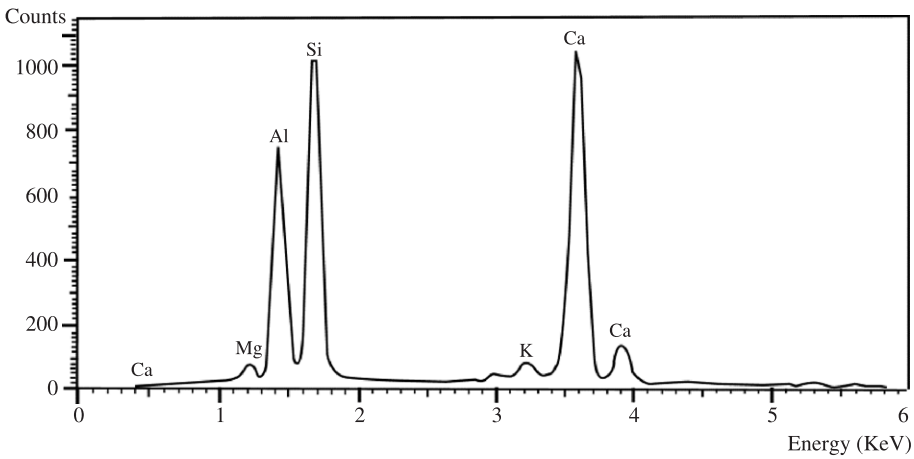

Fig. 8. Example of EDAX analysis of amorphous glassy particle.

Table 8
EDAX analyses of amorphous glassy particles (atomic percent)

Crystal no.	Ca	Si	Al	Mg	Fe	S	K
1	38.06	32.57	26.53	1.04	0.95	0.27	0.57
2	33.07	34.05	29.63	1.10	0.67	0.13	1.36
3	36.79	37.22	16.07	7.41	0.79	0.25	1.47
4	34.08	34.00	29.07	1.38	0.46	0.24	0.78
5	30.50	34.64	31.43	0.69	0.54	0.18	2.01
6	48.02	23.04	22.90	0.97	0.93	0.59	3.55
7	32.50	33.92	30.38	0.65	0.44	0.17	1.96
8	25.16	35.98	33.26	2.02	0.73	0.25	2.61
9	38.98	32.30	24.30	1.56	1.04	0.55	1.28
10	29.07	38.73	25.20	1.75	1.40	0.43	3.42
11	31.19	34.42	30.22	1.11	0.54	0.09	2.44
12	31.85	34.61	29.21	1.22	0.61	0.47	2.03
13	37.33	32.78	27.48	0.89	0.67	0.16	0.32
14	39.57	33.95	25.09	0.57	0.39	0.25	0.18
Mean	34.73	33.73	27.22	1.60	0.73	0.29	1.71

during storage (peaks P). In addition there is a dicalcium silicate phase similar to bredigite (characterised by peaks B at 3.5, 2.76 [overlap with quicklime], 2.71, 2.69, 2.19, 2.04 [overlap with gehlenite] and 1.95 Å) [13]. There are five polymorphs of C_2S from α-C_2S, the highest temperature form, to γ-C_2S, the lowest temperature form. The high-temperature forms can normally only be retained on rapid cooling if stabilised by substituent ions such as Mg. In fact, active belite cements can be formed by doping C_2S and/or by rapid cooling. However, identification of the particular polymorph by XRD is complicated by the fact that the XRD patterns of all the polymorphs are very similar, and the principal group of reflexions all occur in the range 2.6 to 2.8 Å. The TEM studies show that there are two phases intimately associated with each other. One is a C_2S-type phase (probably α'-C_2S) in which there is substantial substitution of Si by Al, and the other is a bredigite-type phase containing excess Mg. According to Taylor [12], α'-C_2S was originally incorrectly identified as bredigite, the latter being considered as nonhydraulic at room temperature, and it is therefore not surprising that XRD data alone are not sufficient to fully characterise the two phases. The XRD peaks labelled B are therefore currently attributed to a combination of both phases. This problem is confirmed by Mosely and Glasser [14], who report that although α'-C_2S and bredigite have different structures, the similarity in their powder patterns makes distinguishing between them difficult. In addition to the crystalline phases described above, there is a small amount of anorthite (CAS_2; peaks A) and possible traces of vaterite/calcite and also quartz.

4.2.2. WSA and WSA–GGBS hydration

Both XRD and DTG analyses were carried out on WSA paste hydrated for 1, 7, 28 and 90 days. Fig. 9 shows the XRD traces of the two extremes, i.e., the raw (as supplied) WSA and the WSA hydrated for 90 days. On hydration, there is a rapid reduction in the principal CaO peaks (2.76, 2.40 and 1.70 Å), which disappear after approximately 1 day, although overlaps with α'-C_2S/bredigite and gehlenite peaks make it difficult to establish the exact time of disappearance. Interestingly, the level of $Ca(OH)_2$ present does not change very significantly on disappearance of the CaO, indicating a rapid consumption of the quicklime. The principal α'-C_2S/bredigite peaks (3.5, 2.76 [overlap], 2.71, 2.69, 2.19 and 1.95 Å) also rapidly decrease in intensity and by 28 days the majority of them have disappeared (Fig. 10). There is no evidence of any decrease in the intensities of the gehlenite and anorthite diffraction peaks, indicating that these phases do not undergo any hydration.

The principal crystalline hydration products of WSA are C_4AH_{13} (peaks C_1) and $C_3A.0.5C\bar{C}.0.5CH.H_{11.5}$ (peaks C_2), identified by the C_1,C_2 broad double peak at around 10° 2θ (8.2 and 7.9 Å, respectively, see Refs. [15,16]). This broad double peak, which is quite pronounced at 1 day, gradually increases in intensity, and at 90 days, the two peaks are clearly differentiated and are relatively strong. The only additional crystalline phase that appears strongly in the diffraction pattern of the hydrated WSA at 90 days is vaterite (3.58, 3.31, 2.73, 2.07, and 1.82 Å), although only traces of vaterite and calcite were apparent in the raw WSA and in the hydrated WSA at 1, 7 and 28 days (see Fig. 10 for

Table 9
Hydraulicity of glassy phase with respect to composition

Oxide	Glassy phase composition (wt.%)	Typical slag[a] composition range (wt.%)	Hydraulicity of glassy phase	
			Requirement[b]	Value
CaO	34.9	30–50	Japan: $\frac{CaO + MgO + Al_2O_3}{SiO_2} \geq 1$	1.7
SiO_2	36.3	27–42		
Al_2O_3	24.8	5–33		
MgO	1.2	1–21	EN 197-1: $\frac{CaO + MgO}{SiO_2} \geq 1$	1.0
Fe_2O_3	1.0	<1		
K_2O	1.4			
SO_3	0.4		F value: $\frac{CaO + CaS + 0.5MgO + Al_2O_3}{SiO_2 + MnO}$ > 1.9 (*good*); 1.5 – 1.9 (*moderate*); < 1.5 (*poor*)	1.7
K_2O/Na_2O		1–3		
S^{2-}		<3		

[a] After Ref. [22].
[b] After Ref. [23].

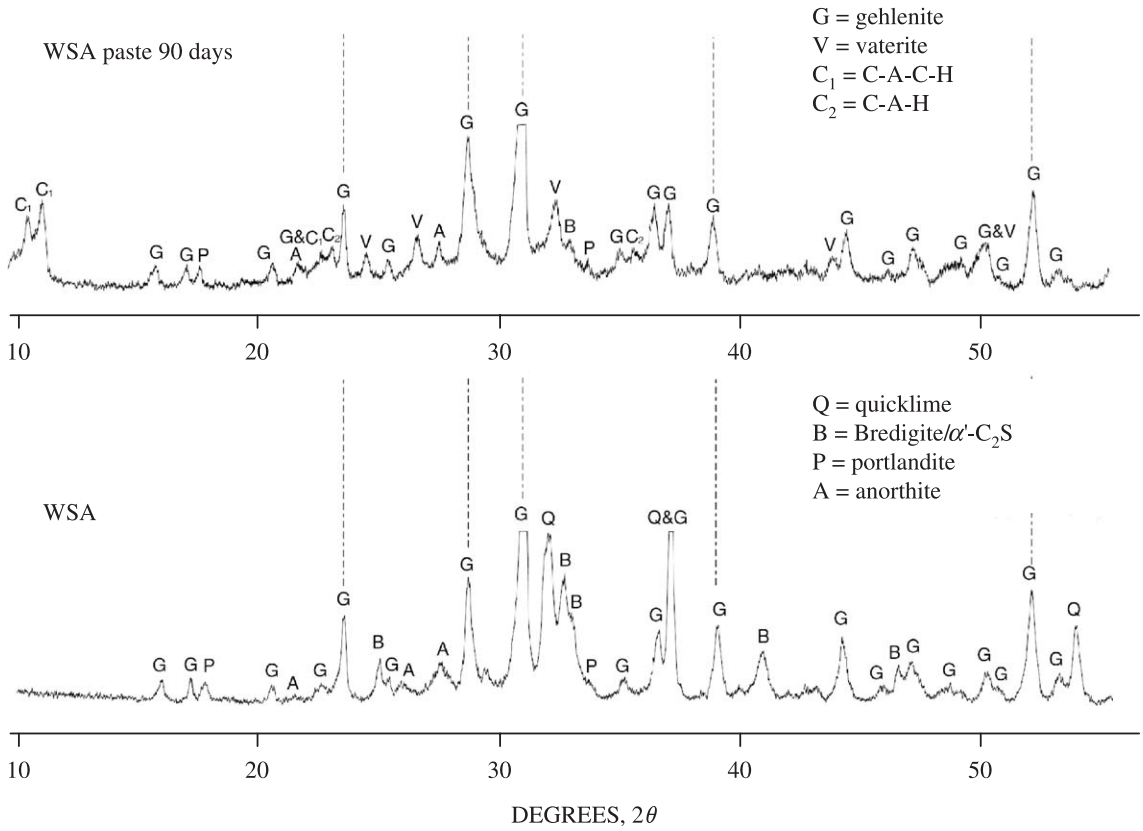

Fig. 9. XRD patterns of WSA and WSA paste cured for 90 days in water.

28 days curing). Hydrated calcium silicates and aluminates are attacked by CO_2 especially when moist, and this is indicated by the appearance of calcite or vaterite in XRD patterns [13]. Thus, the XRD observations suggest that vaterite may in addition be forming from carbonation of the calcium aluminate/silicate phases during long-term curing and subsequent storage.

Fig. 10 shows that when 5% and 10% gypsum are added to the WSA, ettringite rapidly forms on hydration, and the amount appears to increase systematically with increase in gypsum content. Relative to the other crystalline phases present, however, there appears to be little difference in the intensities of the calcium aluminate and carboaluminate diffraction peaks (C_1 and C_2) with or without gypsum, although ettringite formation clearly implies alumina consumption. This may be indicative of accelerated hydration in the presence of gypsum. When WSA is blended with between 30% and 80% GGBS, the crystalline hydration products are the same as for WSA alone (see Fig. 11), that is, $C_3A.0.5C\bar{C}.0.5CH.H_{11.5}$ (peaks C_2) and C_4AH_{13} (peaks C_1), although their proportion decreases with increase in WSA:GGBS ratio, and no additional crystalline products are observed.

Fig. 12 shows the DTG traces of the raw WSA and the WSA hydrated for 1, 7, 28 and 90 days (the DTG traces have been manually offset for clarity). Before hydration, the only weight loss bands present are attributed to CH and $C\bar{C}$ decomposition at around 430 and 620 °C, respectively, and correspond to approximately 0.8 wt.% CH and 3 wt.% $C\bar{C}$ in the WSA, the latter being of the same order as that determined by chemical analysis (see Section 2). On hydration, a strong weight loss band at around 140 °C (attributed to C-S-H gel) is present at 1 day and gradually increases in intensity between 1 and 90 days (Fig. 12). The band has a shoulder at just below 100 °C, which is attributed to the formation of a small amount of ettringite (undetected on the XRD traces), deriving from the small sulphate level (1.05% SO_3; see Table 1) in the WSA. This is supported by the DTG traces of the hydrated WSA containing 0%, 5% and 10% gypsum (Fig. 13) in which the shoulder develops into an increasingly strong weight loss band as the gypsum content increases and correspondingly as the ettringite content increases (Fig. 10). Previous workers have also observed loss of water from ettringite at ~100 °C [16,17]. In addition, during WSA hydration, a shallow weight loss band occurs (Fig. 12) at about 230 °C at 1 day and develops gradually up to 90 days. This is attributed to the dehydration of both the C_4AH_{13} and the $C_3A.0.5C\bar{C}.0.5CH.H_{11.5}$ identified in the XRD traces. Endothermic peaks for these two phases at about 230 °C have also been reported by Frias and Cabrera [18], DeSilva and Glasser [16] and Pera and Ambroise [19] in DTA studies of lime–metakaolin reaction products. The development of the weight loss peak at about 230 °C corresponds

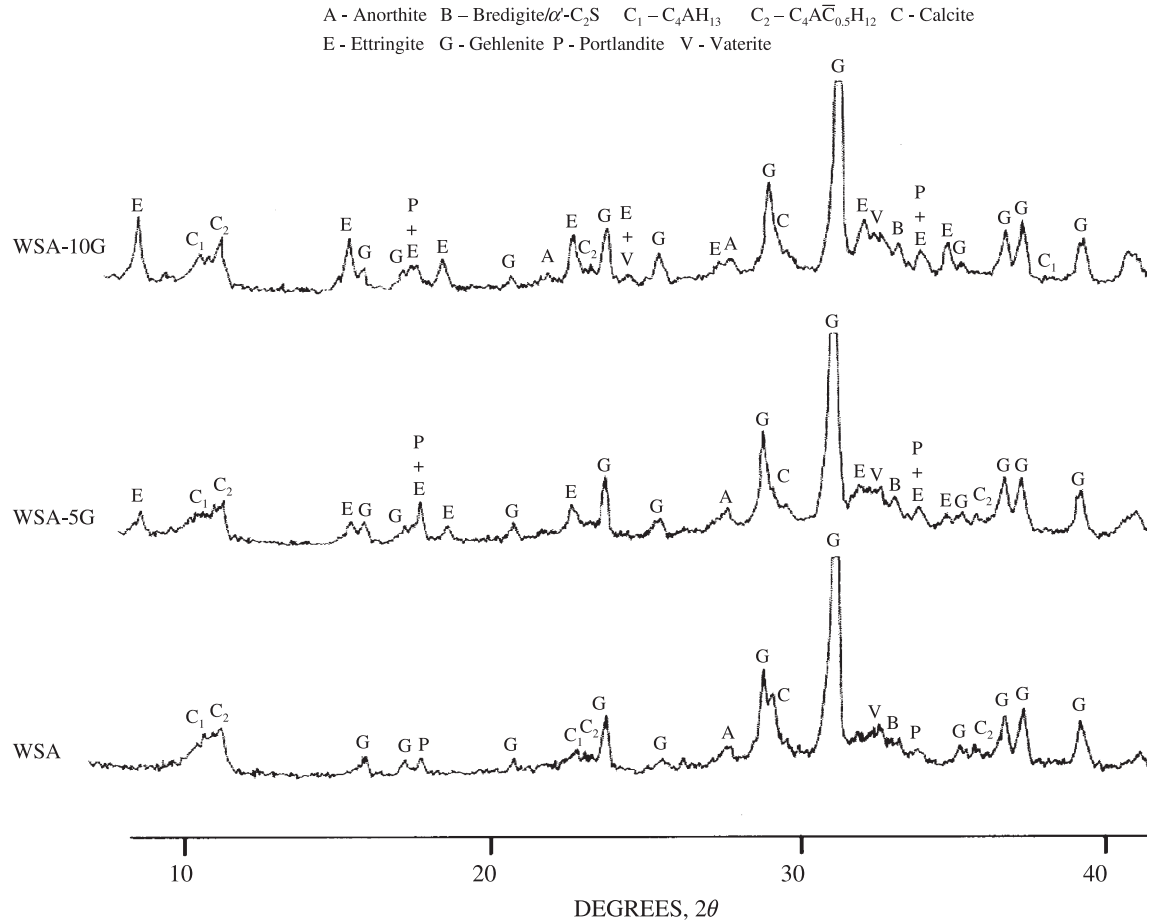

Fig. 10. XRD patterns of WSA, 95% WSA–5% gypsum and 90% WSA–10% gypsum pastes cured for 28 days.

with the appearance of two new peaks at temperatures slightly above and below the $C\bar{C}$ decomposition peak (which occurs at around 620 °C). The growth of the two peaks is associated with a reduction in the size of the $C\bar{C}$ decomposition peak. These two new peaks are attributed to the loss of CO_2, possibly from further decomposition of $C_3A.0.5C\bar{C}.0.5CH.H_{11.5}$, which loses its water at around 230 °C or from decomposition of the developing vaterite phase. Also after 7 days, there is the development of a minor weight loss peak at about 180 °C, which is particularly apparent at 28 days. Reports by numerous authors [18,20,21] in similar systems have attributed this peak (between 180 and 220 °C) to C_2ASH_8, although in the current work there is no evidence of crystalline C_2ASH_8 on XRD traces. It should be noted that there is still CH present even after 90 days, and the amount of CH present does not show any significant reduction beyond 7 days (see Table 10).

Fig. 14 compares the DTG traces of the 28-day cured GGBS, WSA:GGBS (compositions 20:80 to 100:0) and PC pastes. At 28 days, the principal effect of the GGBS with respect to hydrate phase development appears to be one of dilution, in that the two most clearly defined peaks at 140 °C (C-S-H) and 430 °C (CH) proportionately reduce as the GGBS content increases, as do the crystalline aluminate and carboaluminate hydrate phases apparent in the XRD observations (Fig. 11).

4.2.3. Discussion

It is of interest that the products identified during WSA hydration in the current work are very similar to those reported by Pera and Amrouz [2] (i.e., C-S-H, $C_4A\bar{C}H_{12}$ and CH) when wastepaper sludge, which has been calcined for 2 to 5 h at 700 °C, is hydrated. However, the hydration products in the latter derive from the reaction between MK, CH, $C\bar{C}$ and H, whereas in the current work the WSA, which has been produced at much higher temperatures, does not contain any observable amounts of MK. It does, however, contain a hydraulic crystalline dicalcium silicate phase (α'-C_2S stabilised mainly with Al and small levels of Mg) intimately mixed with a bredigite-type phase (rich in Mg and deficient in Si plus small levels of Al), which may or may not be hydraulic. There are also small amounts of calcium aluminosilicate glass of variable composition that probably possess some latent hydraulicity. Fig. 15 locates the composition of WSA and the compositions of the glassy phase, the α'-C_2S phase and the gehlenite phase on the ternary $CaO–SiO_2–Al_2O_3$ diagram. It should be noted that the compositions of the phases present in WSA (i.e., quicklime,

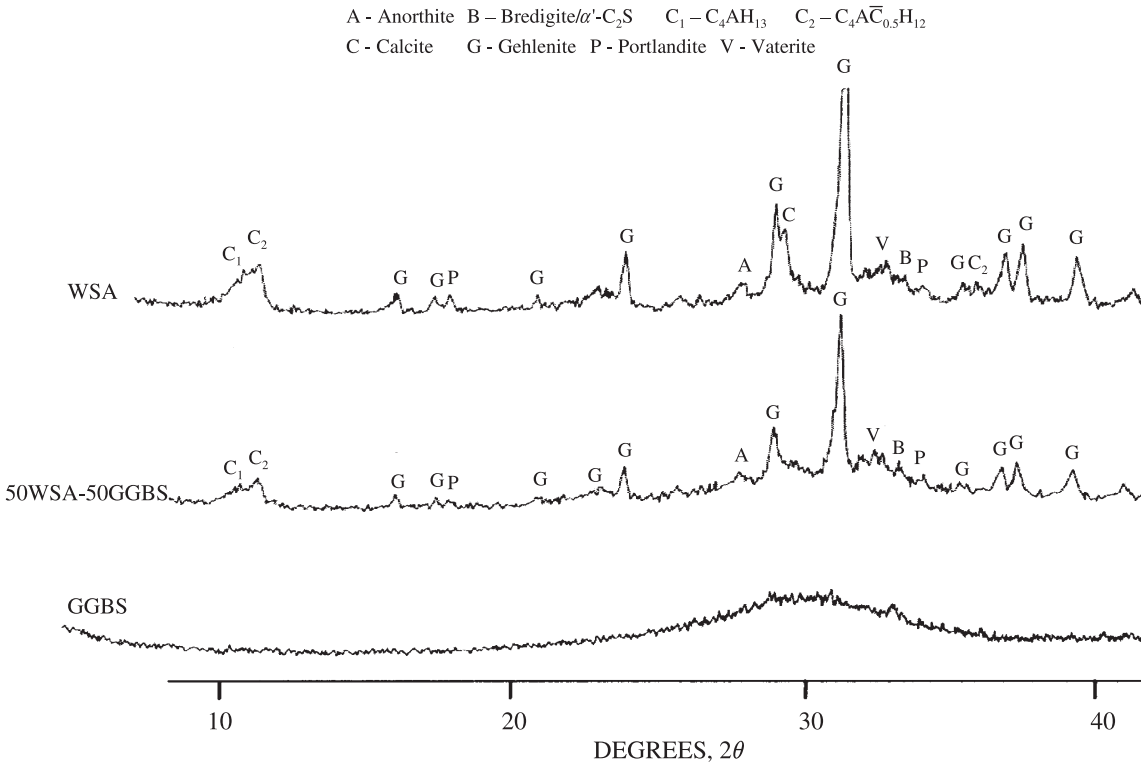

Fig. 11. XRD patterns of WSA, 50% WSA–50% GGBS and GGBS pastes cured for 28 days.

α'-C_2S, gehlenite, glassy phase and probably the small amount of anorthite) all lie on a straight line that cuts the Al_2O_3–SiO_2 axis slightly on the silica-rich side of metakaolin (AS_2). This is not surprising in that WSA is formed from reaction between CaO and AS_2 and the fact that the intersection occurs on the silica-rich side of AS_2, may be a result of silica contamination from the fluidised bed. Clearly the bredigite-type phase, which is a Ca-Si-Mg phase containing a small amount of Al, will not lie in this plane but will lie in the plane CaO–bredigite–AS_2 within the CaO–SiO_2–Al_2O_3–MgO system. In addition, it should be noted that the glass composition is close to the ternary gehlenite–

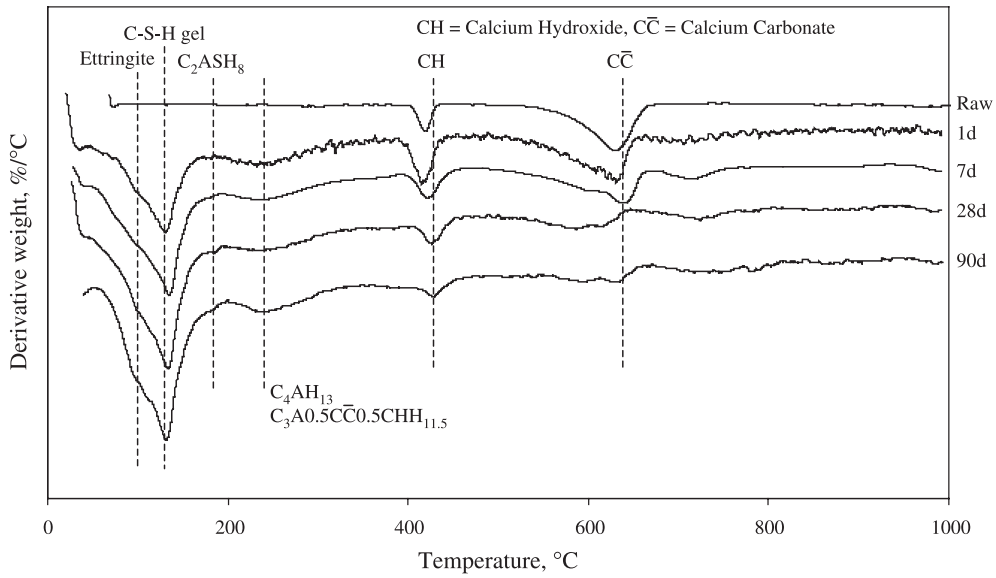

Fig. 12. DTA result of raw WSA and WSA pastes at 1, 7, 28 and 90 days.

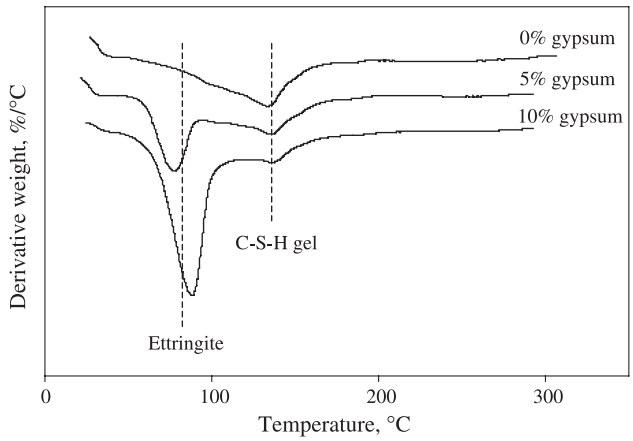

Fig. 13. DTA of raw WSA with 0%, 5% and 10% gypsum at 28 days.

anorthite–αCS eutectic at 1265 °C, which is somewhat higher than the estimated maximum temperature in the combustion process. However, the presence of Mg, and especially K, in the glass is likely to reduce the eutectic temperature further.

The XRD of WSA paste shows that α'-C_2S/bredigite reflexions virtually disappear from the XRD pattern during curing, the corresponding XRD analysis confirms formation of calcium aluminate/carboaluminate hydrates and the TG observations indicate formation of C-S-H gel. It should of course be noted that the small crystals comprise two distinct phases, and the degree to which the bredigite-type phase hydrates is not known. Hydration of the α'-C_2S would be expected to form C-S-H gel and CH, but as the α'-C_2S also contains substantial amounts of Al (Table 6), not all of the Al would be accommodated in the gel and would therefore be available for formation of aluminate/carboaluminate hydrates. It is less clear what the destination of the small level of Mg would be (i.e., whether a magnesium silicate gel would form or whether the magnesium would be incorporated in a hydrotalcite-type phase as it is in hydrated GGBS).

The second component in the WSA that might be expected to react with water, particularly in an alkaline environment, is the calcium aluminosilicate glass. However, the composition of the glass indicates (Table 9) relatively low hydraulicity, therefore relatively slow reaction might be expected in the alkaline environment provided by the CH which would again produce C-S-H gel and aluminate/carboaluminate hydrates. When gypsum ($C\bar{S}H_2$) is present, ettringite would preferentially form in both systems, and the presence of gypsum might also be expected to accelerate the hydration of the hydraulic phases and activate the hydration of the glass.

Although there is about 5 wt.% CaO initially present in the WSA (which on hydration will hydrate to CH) and α'-C_2S hydration will produce even more CH, the CH content of the hydrating WSA changes very little with curing time (Table 10). The CH content is only 3 wt.% at 1 day and drops slightly between 1 and 7 days. It then increases slightly between 7 and 90 days to a value of 3.5 wt.%. However, the reactions involving hydration of the amorphous calcium aluminosilicate glass would be expected to involve consumption of lime, particularly as the glass has a relatively low Ca/Si ratio, which may explain why there is no continuous and significant increase in CH content with curing time.

When water is added to WSA, very rapid reaction and setting occur [6] and workability is poor. Based upon the analyses of the reactants and the reaction products, it is proposed that the initial rapid reaction and setting is strongly influenced by the hydration of CaO to $Ca(OH)_2$. In addition, the hydration of α'-C_2S may also contribute to the initial set. However, although substantial hydration clearly occurs within the first 24 h and hydration is well advanced by 28 days, the strength that develops for hydrated WSA paste alone is very small (Figs. 1 and 2). This is not the case when the WSA is blended with GGBS. The very low strength of

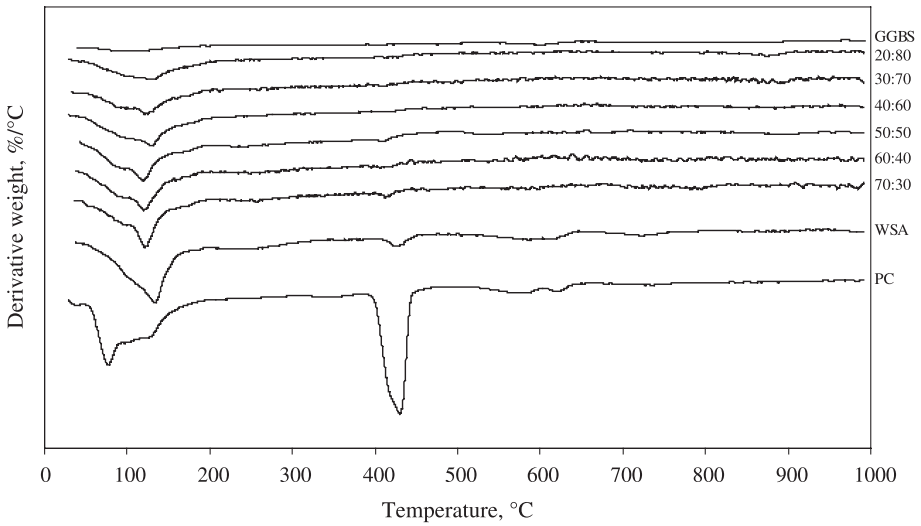

Fig. 14. DTA of GGBS, WSA–GGBS, WSA and PC pastes at 28 days.

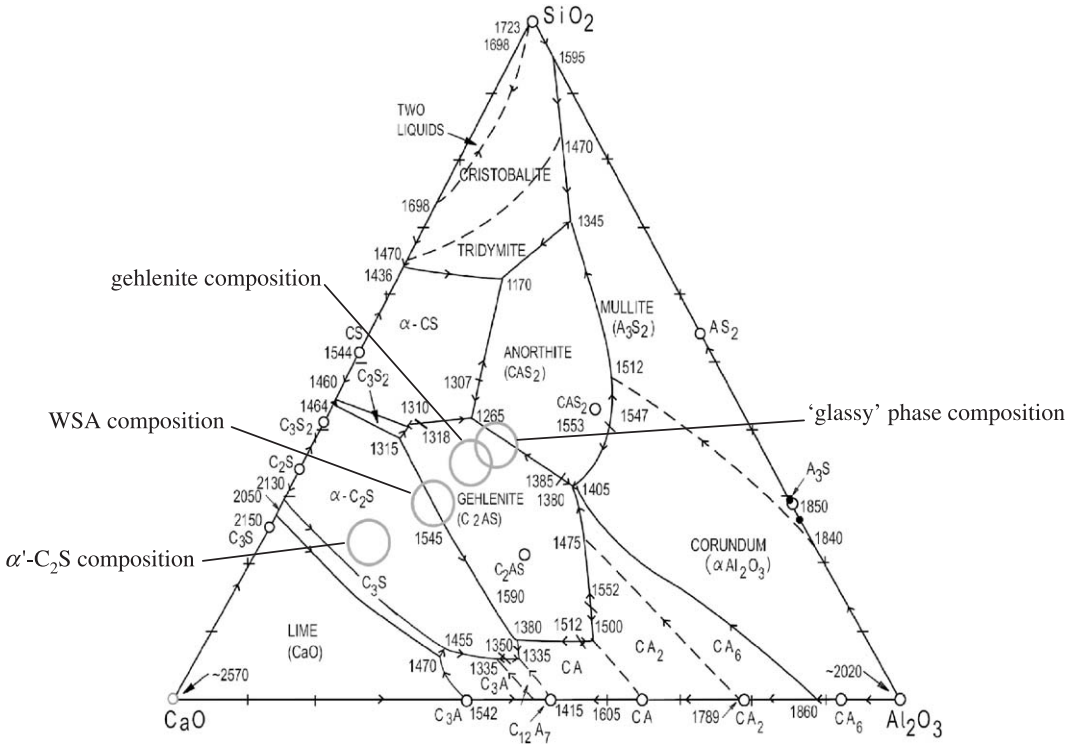

Fig. 15. The system $CaO-Al_2O_3-SiO_2$ (after Taylor [12]).

WSA paste is directly related to its high level of coarse porosity. That coarse porosity arises due to a degree of unsoundness of the WSA because of expansion caused by CaO hydration after setting. The hydration of other components in the WSA may also contribute to the unsoundness. When WSA is blended with GGBS, however, the initial porosity of the resultant hardened paste is much reduced as is its expansion, and substantial pore refinement is achieved. This results in much higher strengths. It is suggested that the GGBS has two roles in effecting this improvement in pore structure and performance. Firstly, it dilutes the system, thus reducing the amount of expansive product per unit of available pore space and also increasing the effective water to WSA ratio, enabling a greater degree of CaO hydration to occur before setting. Hence, the degree of disruption to the hardened fabric is minimised and the overall expansion reduced. Secondly, it mitigates the expansion by providing a surface upon which lime can be adsorbed and subsequently interact activating slag hydration in the enhanced pH environment. The slow hydration of the GGBS beyond the first few days coupled with any further hydration of the WSA components provides significant strength enhancement up to at least 90 days. Without the GGBS, the pore structure initially developed on setting is of such a coarse nature that any further hydration of the components in the WSA is insufficient to produce significant pore refinement and hence strength enhancement.

Table 10
Calcium hydroxide (CH) percentage in WSA pastes at different periods of curing

Curing period (days)	0	1	7	28	90
Calcium hydroxide (CH; %)	0.837	3.088	2.849	3.042	3.493

Kinuthia et al. [6] and Veerappan [24] have demonstrated that it is possible to produce low-grade concrete using PC–WSA–GGBS blends as binders, and binders are being further developed for applications in the production of concrete blocks [24]. However, such applications require a basic understanding of the nature of the material and its properties, which was one of the objects of this paper. Current work also in progress includes investigations of the setting times and heat evolution of fresh pastes and porosity and pore size distributions and sulphate resistance of cured pastes. The results in this paper therefore form a contribution to a much more extensive programme of research on WSA.

5. Conclusions

The following conclusions may be drawn from this study:

- Wastepaper sludge (which comprises an intimate mixture of finely divided calcium carbonate and kaolin) when heated rapidly (3–5 s) up to a maximum temperature of 1200 °C and then cooled rapidly (3–5 s) to 200 °C, forms a fine ash (WSA), which has cementitious properties.

- The ash consists of several different crystalline phases, the principal ones being gehlenite, quicklime and α'-C_2S/bredigite, together with small amounts of hydrated lime and anorthite and traces of calcite, vaterite and quartz. There is also a significant amorphous component consisting of calcium aluminosilicate glass spheres with varying calcium levels but with Al/Si ratios varying over a relatively narrow range. There is no evidence from TEM studies of any residual metakaolin.
- Paste formed from WSA–water mixtures shows rapid setting and very low rates of strength development, and the strengths achieved are very small. The rapid setting is attributed to hydration of CaO to $Ca(OH)_2$. In addition, the hydration of α'-C_2S/bredigite may contribute to the rapid initial set. The low strengths are attributed to the early development of a highly porous paste with a coarse pore structure as a result of the paste unsoundness, which derives principally from the expansive nature of quicklime hydration. Subsequent slow hardening of the paste is attributed to continued hydration of the hydraulic components of the WSA, including the amorphous glassy phase.
- The principal products of hydration of WSA are C_4AH_{13}, $C_3A.0.5C\bar{C}.0.5CH.H_{11.5}$ and C-S-H gel.
- Pastes formed from WSA–GGBS blends, in contrast to WSA paste, show less rapid setting and increased strength development. The optimum blend composition to give maximum strength is 50% WSA–50% GGBS, and after 90 days, pastes manufactured from this blend exhibit compressive strengths close to 50% of those from an equivalent Portland cement paste.
- The improved strength development of WSA–GGBS pastes relative to WSA paste is attributed to:
  i) dilution of the system by the GGBS, thus reducing the amount of expansive product per unit of available pore space and minimising the degree of disruption to the hardened fabric by reducing the overall expansion;
  ii) increasing the effective water to WSA ratio, enabling a greater degree of CaO hydration to occur before setting;
  iii) mitigation of the expansion by providing a surface upon which lime can be adsorbed and subsequently interact, thus activating slag hydration in the enhanced pH environment;
  iv) slow hydration of the GGBS beyond the first few days coupled with any further hydration of the WSA.

Further research is being undertaken as a part of the research programme [24] on the properties of the WSA–GGBS binders (including durability) to establish the practical application in the production of low grade concrete.

Acknowledgements

The authors are grateful to EPSRC for providing the research grant on this research programme and would like to thank Aylesford Newsprint and The Cementitious Slag Makers Association for providing funding and materials for the project. The authors are grateful to Mr. Govindarajan Veerappan, who is carrying out the research and development work on low-level PC with WSA–GGBS blends for applications including concrete block production, for helpful discussion. The authors would also like to thank Steve York at the University of Warwick for assisting with the electron microscopy, Dr. Kath Liddell at the University of Newcastle for the XRD work and the head and technical staff of the School of Technology, University of Glamorgan for their technical assistance.

References

[1] E. Kilby, Current statistics on recovered paper, in: R.K. Dhir, M.C. Limbachiya, M.D. Newlands (Eds.), Proceedings of an International Symposium on Recovery and Recycling of Paper, Dundee 2001, Thomas Telford, London, 2001, pp. 93–104.
[2] J. Pera, A. Amrouz, Development of highly reactive metakaolin from paper sludge, Adv. Cem. Based Mater. 7 (1998) 49–56.
[3] J.B. McNicholas, P.J. Webster, New construction materials from paper waste residues, Br. Ceram. Trans. 97 (4) (1998) 191–193.
[4] W.M.J. Frederick, K. Issa, J.R. Lundy, W.K. O'Connor, K. Reis, A.T. Scott, S.A. Sinquefield, V. Sricharoenchaikul, C.A. Van Vooren, Energy and materials recovery from recycled paper sludge, Tappi J. 79 (6) (1996) 123–131.
[5] H. Ishimoto, T. Origuchi, M. Yasuda, Use of papermaking sludge as new material, J. Mater. Civ. Eng., November (2000) 310–313.
[6] J.M. Kinuthia, M. O'Farrell, B.B. Sabir, S. Wild, A preliminary study of the cementitious properties of wastepaper sludge ash–ground granulated blastfurnace slag (wsa–ggbs) blends, in: R.K. Dhir, M.C. Limbachiya, M.D. Newlands (Eds.), Recovery and Recycling of Paper, Proceedings of the International Symposium, University of Dundee, Thomas Telford, London, 2001, pp. 93–104.
[7] S. Salvador, Pozzolanic properties of flash-calcined kaolinite: a comparative study with soak-calcined products, Cem. Concr. Res. 25 (1) (1995) 102–112.
[8] BS EN 196-2, Methods of Testing Cement: Part 2. Chemical Analysis of Cement, BSI, European Committee for Standardization (CEN), Brussels, 1995.
[9] BS 12, Specification for Portland Cement, BSI, British Standards (BS), London, 1996.
[10] BS EN 196-3, Methods of Testing Cement: Part 3. Determination of Setting Time and Soundness, BSI, European Committee for Standardization (CEN), Brussels, 1995.
[11] BS EN 196-1, Methods of Testing cement: Part 1. Determination of Strength, BSI, European Committee for Standardization (CEN), Brussels, 1995.
[12] H.F.W. Taylor, Cement Chemistry, 2nd ed., Thomas Telford, London, 1997, p. 19, 43.
[13] H.F.W. Taylor, The Chemistry of Cements, vol. 2, Academic Press, London, 1964.
[14] D. Mosely, F.P. Glasser, Identity, composition and stability of bredigite and phase T, Cem. Concr. Res. 11 (1981) 559–565.
[15] V.L. Bonavetti, V.F. Rahhal, E.F. Irassar, Studies on the carboaluminate formation of limestone filler-blended cements, Cem. Concr. Res. 31 (6) (2001) 853–859.
[16] P.S. DeSilva, F.P. Glasser, Hydration of cement based on metakaolin thermochemistry, Adv. Cem. Res. 3 (12) (1990) 167–177.
[17] L. Zhang, F.P. Glasser, Critical examination of drying damage to cement pastes, Adv. Cem. Res. 12 (2) (2000) 79–88.
[18] M. Frias, J. Cabrera, Influence of MK on the reaction kinetics in MK/

lime and MK-blended cement systems at 20 °C, Cem. Concr. Res. 31 (4) (2001) 519–527.
[19] J. Pera, J. Ambroise, Pozzolanic properties of metakaolin obtained from paper sludge, in: V.M. Malhotra (Ed.), Sixth CANMET/ACI, Conference On Fly Ash, Silica Fume, Slag and Natural Pozzolans in Concrete (SP178-52), Bangkok, 1998, pp. 1007–1020.
[20] M.A. Serry, A.S. Taha, S.A.S. El-Hemaly, H. El-Didamony, Metakaolin–lime hydration products, Thermochim. Acta 79 (1983) 103–110.
[21] M. Murat, Hydration reaction and hardening of calcined clays and related minerals, I—preliminary investigation on metakaolinite, Cem. Concr. Res. 13 (1983) 259–266.
[22] I. Odler, Special inorganic cements, Modern Concrete Technology, vol. 8, E & FN Spon, London, 2000, p. 114.
[23] E. Lang, Blastfurnace cements, in: J. Bensted, P. Barnes (Eds.), Structure and Performance of Cements, 2nd ed., Spon, London, 2002, pp. 310–323.
[24] G. Veerappan, The development of low cost, low energy cement from waste, MPhil/PhD transfer report, University of Glamorgan, Pontypridd, December 2001.